

Medical Applications with Synchrotron Radiation in Japan

Tohoru Takeda,^{a*} Yuji Itai,^a Kazuyuki Hyodo,^b Masami Ando,^b Takao Akatsuka^c and Chikao Uyama^d

^a*Institute of Clinical Medicine, University of Tsukuba, Tsukuba 305, Japan,* ^b*KEK, Tsukuba 305, Japan,* ^c*Faculty of Engineering, Yamagata University, Yamagata 902, Japan,* and ^d*National Cardiovascular Centre, Suita 565, Japan. E-mail: ttakeda@md.tsukuba.ac.jp*

(Received 4 August 1997; accepted 2 December 1997)

In Japan, various medical applications of synchrotron X-ray imaging, such as angiography, monochromatic X-ray computed tomography (CT), radiography and radiation therapy, are being developed. In particular, coronary arteriography (CAG) is quite an important clinical application of synchrotron radiation. Using a two-dimensional imaging method, the first human intravenous CAG was carried out at KEK in May 1996; however, further improvements of image quality are required in clinical practice. On the other hand, two-dimensional aortographic CAG revealed canine coronary arteries as clearly as those on selective CAG, and coronary arteries less than 0.2 mm in diameter. Among applications of synchrotron radiation to X-ray CT, phase-contrast X-ray CT and fluorescent X-ray CT are expected to be very interesting future applications of synchrotron radiation. For actual clinical applications of synchrotron radiation, a medical beamline and a laboratory are now being constructed at SPring-8 in Harima.

Keywords: coronary angiography; fluorescent X-ray computed tomography; phase-contrast X-ray computed tomography; scattered X-ray computed tomography; monochromatic X-rays; diagnostic radiology.

1. Introduction

In Japan, various medical applications of X-ray imaging with synchrotron radiation, such as angiography, monochromatic X-ray computed tomography (CT), radiography and radiation therapy, are being developed (Table 1). In particular, intravenous coronary arteriography (CAG) is quite an important and prospective clinical application of synchrotron radiation. In Japan, a two-dimensional imaging method with synchrotron radiation has been combined with various angiographic approaches, such as intravenous CAG, aortographic CAG and selective angiography in animal studies. In May 1996, the first human intravenous CAG was carried out at KEK.

X-ray computed tomography is an important diagnostic modality. Using the excellent properties of synchrotron radiation, several synchrotron radiation X-ray CT techniques have been examined, including spectrum-subtraction CT and scattered CT. Among applications of synchrotron radiation to computed tomography, phase-contrast X-ray CT and fluorescent X-ray CT are expected to be very interesting future applications of synchrotron radiation. In this paper, the present state of synchrotron medical applications in Japan is described.

2. Coronary angiography

Coronary arterial disease is one of the most dominant diseases in industrial countries. Selective CAG is the 'gold standard' among diagnostic methods for this disease; however, fatal accidents occasionally occur (0.14% examination⁻¹) during direct coronary arterial catheterization (Pepine *et al.*, 1991). In 1981, Rubenstein *et al.* (1981) speculated that an intravenous *K*-edge energy-subtraction CAG with synchrotron radiation would be a safer and more easily repeatable method of imaging the coronary arteries. Using a line-scan method, human studies have been performed in the USA (Rubenstein *et al.*, 1986; Chapman *et al.*, 1995) and Germany (Dix *et al.*, 1992; Dix, 1995).

In Japan since 1983, two-dimensional-sensing intravenous CAG with synchrotron radiation (2D-CAG) has been under development (Akisada *et al.*, 1986; Hyodo *et al.*, 1991). There are potential advantages of a two-dimensional-sensor imaging technique over a line-scan method for clinical diagnosis, since ventricular wall motion, the coronary artery structures and coronary flow can be demonstrated as in conventional cine images.

Three different techniques for *K*-edge energy exchange have been developed, namely the oscillatory method (Akisada *et al.*, 1986; Fukagawa *et al.*, 1989; Takeda *et al.*,

Table 1

Medical applications with synchrotron radiation.

Angiography	
(a) Coronary angiography	Intravenous coronary angiography Aortographic coronary angiography Selective arteriography
(b) Microangiography	
Computed tomography	
(a) Transmission types	High-spatial-resolution CT High-contrast-resolution CT Three-dimensional CT by fluorescent X-ray source
(b) Fluorescent scanning CT	
(c) Scattering CT (Compton and Thomson)	
(d) Phase contrast X-ray CT	
Radiography	Mammography, chest radiography
Radiation therapy	

1990), the filter method (Umetani *et al.*, 1993; Takeda, Itai, Yoshioka *et al.*, 1994), and the use of a dual linearly polarized synchrotron radiation beam from an elliptical multipole wiggler (Hyodo *et al.*, 1994). In the oscillatory method, images above and below the iodine *K*-edge are obtained by changing the angle of the monochromator, whereas in the filter method a small filter filled with iodine filtrates the beam with mixed X-ray energy, and subtraction between the filtered and non-filtered images forms coronary images. If a dual linearly polarized synchrotron radiation beam is monochromated above and below the *K*-edge energy by two monochromators, then images with each energy are obtained simultaneously.

2D-CAG studies suggested that *K*-edge energy subtraction might not be necessary for intravenous CAG because coronary arteries could be revealed almost completely without subtraction (Takeda, Itai *et al.*, 1995; Ohtsuka *et al.*, 1997). Accordingly, a recent study of 2D-CAG in Japan was performed using monochromatic X-rays just above the iodine *K*-edge. In intravenous CAG, the coronary arteries overlapping on cardiac chambers and the dilution process of contrast material determined by the cardiac function reduced the visibility of arteries. To overcome these problems, aortographic CAG was examined in dogs (Takeda, Umetani *et al.*, 1997, 1998; Umetani *et al.*, 1996).

In addition, micro-angiographic approaches using selective angiographic procedures have been attempted (Mori *et al.*, 1994).

2.1. Experimental methods and materials for monochromatic 2D-CAG

2.1.1. Animal experiments. A 2D-CAG system with synchrotron radiation was constructed at the wiggler beamline of the Photon Factory in Tsukuba. This system consists of an Si(311) monocrystal, a fluorescent plate, an avalanche-type pick-up tube camera, and an image-acquisition system (Fig. 1). A 40×70 mm monochromatic X-ray beam was obtained by asymmetric reflection. The beam energy was adjusted to just above the iodine *K*-edge (33.32 keV). X-ray video images were digitized in a

512×512 pixel matrix with a 12-bit depth. The image-acquisition interval was set at 16.7 ms. The storage ring was operated at 2.5 GeV with a typical current of approximately 300 mA. The monochromatic X-ray flux in front of the object was about 1.6×10^9 photons $s^{-1} mm^{-2}$.

Dogs (average weight 12 kg) were anesthetized. A 5 F catheter was inserted into the aorta, and a 7 F catheter was also inserted into the pulmonary artery. Contrast material (Iomeprol 350, 0.90 ml kg^{-1}) was injected by the injector at a rate of 10 ml s^{-1} . Present experiments were approved by the Medical Committee for the Use of Animals in Research at the University of Tsukuba, and they are executed under the guidelines of the American Physiological Society.

2.1.2. Human studies. A 2D-CAG system with synchrotron radiation for human studies was constructed at the 21-pole wiggler beamline BL-NE1 of the Tristan accumulation ring in Tsukuba. This system consists of an Si(311) single-crystal monochromator, an image-intensifier video camera, X-ray shutters and an image-acquisition system. Contrast material (Iomeprol 400, 40 ml) was injected by an injector at a rate of 20 ml s^{-1} .

2.2. Results of animal experiments

Typical images of canine coronary arteries obtained by intravenous CAG and aortographic CAG are shown in Fig. 2.

2.2.1. Intravenous approach. Contrast material was injected into the pulmonary artery to increase the concentration of contrast material. In images obtained from a dog with a slightly reduced cardiac function, only the branches of the left anterior descending coronary arteries (LAD) and right coronary artery could be observed at end-systole (Fig. 2a). For the case of a good cardiac function, however, almost all coronary arteries could be demonstrated clearly (Fig. 2b).

2.2.2. Aortographic approach. Just after intravenous CAG, aortographic CAG was performed on the same dogs with the same view angle. The injected contrast material filled the aorta and coronary arteries, and soon afterwards contrast material was washed out from the aorta. Cinematic images revealed the time course of coronary flow. Almost all coronary arteries could be imaged clearly without significant influences of the reduced cardiac

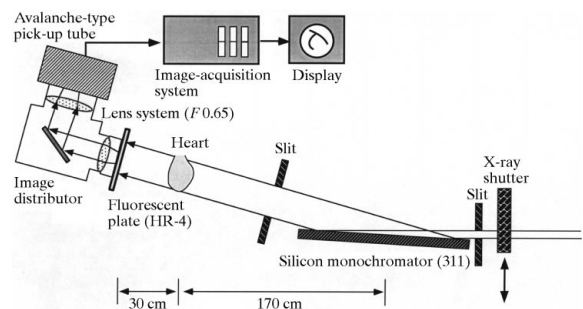


Figure 1
Schematic diagram of the 2D-CAG system.

function (Figs. 2c and 2d). Coronary arteries overlapping on the aorta could also be described clearly after contrast material had been washed out from the aorta.

Using a vasodilatory drug such as Nitrol, about 50% dilatation of coronary arteries could be clearly observed (Fig. 3). The diameter of the main coronary artery was estimated to be about 1.8 mm, while the distal branches of coronary arteries were less than 0.2 mm in diameter. The ratio of contrast dilution was quantified as about 2.4–3.4 on aortography.

2.3. Results of the human study

Four patients were examined by two-dimensional intravenous CAG. Two patients were diagnosed with significant coronary stenosis; however, further improvement of the image quality is required for clinical practice.

2.4. Discussion on synchrotron radiation angiography

In the USA, Germany and Japan, synchrotron radiation coronary angiographic studies have been conducted by the intravenous approach to image coronary structures as a safe and easily repeatable method. For this purpose, *K*-edge energy subtraction with synchrotron radiation was developed (Rubenstein *et al.*, 1981). Nevertheless, prior to its actual clinical use, many problems, such as the low

concentration of contrast material in patients with reduced cardiac function, and image overlapping of the coronary arteries on the cardiac chambers and various vessels, must be overcome. These problems were also observed in human studies with two-dimensional intravenous CAG.

2.4.1. Aortographic approach. Previously, the aortographic approach for coronary arterial diagnosis was taken when conventional selective CAG was not successful for technical reasons related to arteriosclerotic changes. However, only the main coronary arteries were visualized by this method. Thus, this approach has been abandoned as a diagnostic procedure for coronary arteries. However, even when the cardiac function is reduced, canine experiments indicate that aortographic CAG with synchrotron radiation provides clear images of the coronary arteries, because the image contrast is improved by the synchrotron radiation method (two times or more).

The aortographic procedure is much safer than selective CAG, as the overall frequency of fatal accidents on selective CAG is about 0.14%, while that in aortographic CAG is about 0.025% (Hessel, 1983). In addition, a remarkable reduction of X-ray exposure to clinical staff is also expected. This means that aortographic CAG might be used as a highly reliable screening procedure replacing selective CAG (Takeda, Umetani *et al.*, 1997, 1998). In contrast, intravenous CAG might be suitable only for follow-up studies in PTCA and CABG, because of insufficient image quality for precise clinical diagnosis and the image overlapping problems.

For actual clinical applications of synchrotron radiation, a medical beamline and a laboratory are currently being constructed at SPring-8 in Harima.

2.4.2. X-ray exposure. In the animal experiments, the X-ray dose in front of the sensor to obtain one image was about 1.67 mR (3×10^5 photons mm^{-2} frame $^{-1}$). Obtaining the same quality of images in human studies, the entrance surface dose to the patient would be 1.67 R (16.7 mSv). In intravenous CAG with synchrotron radiation, the maximal allowable total entrance surface dose to

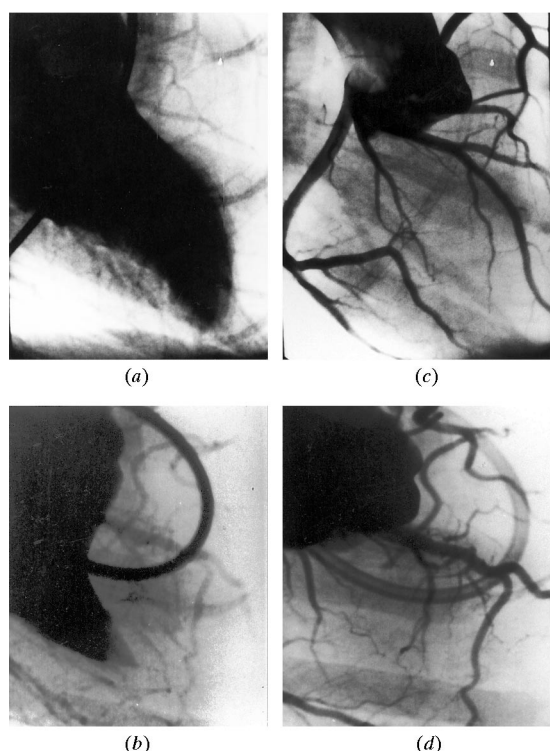


Figure 2
2D-CAG images obtained by intravenous and aortographic procedures. (a) Only the branches of the left anterior descending coronary arteries and right coronary artery of dog could be observed at end-systole due to the reduced cardiac function. (b) Many coronary arteries could be demonstrated clearly due to a good cardiac function. (c), (d) All coronary arteries could be imaged clearly without influences of reduced cardiac function.

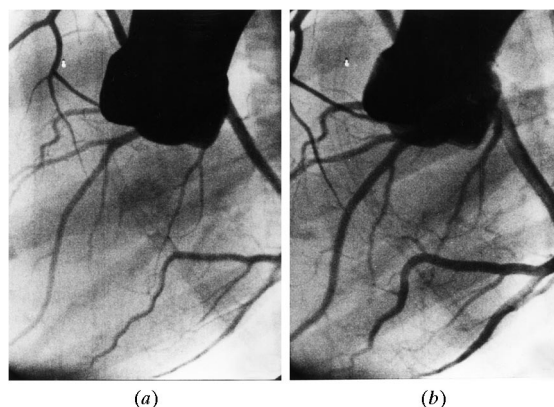


Figure 3
Aortographic CAG (a) before and (b) after a vasodilatory drug such as Nitrol. About 50% dilatation of coronary arteries could be observed.

the subject is 350 mSv for one projection (Rubenstein *et al.*, 1986). In this aortographic CAG, the total number of frames would thus be limited to about 21.

By the non-subtraction procedure, X-ray exposure to the patients (Motz & Danos, 1978) would be reduced by using a much higher X-ray energy than that just above the *K*-edge energy without reducing the image contrast (Fig. 4).

3. Computed tomography with synchrotron radiation

X-ray computed tomography with a conventional X-ray source, *i.e.* an X-ray tube, is an important diagnostic modality in the medical field. In 1983, Grodzins proposed synchrotron radiation as an alternative X-ray source for CT (Grodzins, 1983). The great advantage of synchrotron radiation for CT is a high X-ray flux with a broad-band energy spectrum to adjust suitable monochromatic X-rays and linear polarization. Using these properties, various types of CT are now being developed (Table 1).

3.1. Transmission CT

Since 1991 we have been constructing a transmission X-ray CT system to visualize fine structures in living tissue and detect specific contrast materials for quantitative functional evaluation, such as that of the regional blood flow in various anatomical structures.

3.1.1. *High-spatial-resolution X-ray CT.* High-spatial-resolution CT with synchrotron radiation has already been applied in industrial and materials science investigations. High-spatial-resolution images of bony structures have been obtained (Bonse & Busch, 1996). In Japan, monochromatic X-ray CT was produced to facilitate examina-

tion of the microstructures of material and biological specimens. It provides excellent contrast and has a spatial resolution capacity ranging from 2 to 100 μm . In a preliminary experiment, images from a live rat were obtained at 36 μm slice thickness and 33.2 keV X-ray energy (Takeda, Itai, Hayashi *et al.*, 1994). The nasal cartilage, skull and teeth of a live rat were clearly demonstrated with 36 μm spatial resolution (Fig. 5).

3.1.2. *High-contrast-resolution X-ray CT.* High-contrast X-ray CT with synchrotron radiation is being developed for detection of non-radioactive contrast agents at low concentrations for application in clinical diagnosis. Initial experiments using an imaging plate (IP) as an X-ray detector and an Si(111) channel-cut monochromator showed that the minimal detectable concentration of iodine was about 500 $\mu\text{g ml}^{-1}$ on the image above the *K*-edge due to the poor dynamic range of the IP reader (Takeda *et al.*, 1992; Zeniya *et al.*, 1997). Recently, an acrylic phantom with 1 mm holes filled with 200 $\mu\text{g ml}^{-1}$ iodine solution was demonstrated with a 1 mm slice thickness using a linear array detector. However, this minimal detectable concentration of iodine is about six times higher than the expected value of 35.3 $\mu\text{g ml}^{-1}$ because of the high dark current of the detector (Itai *et al.*, 1995; Kazama *et al.*, 1997; Takeda, Kazama *et al.*, 1998). Thus, the use of a CCD detector, which is cooled by liquid nitrogen to improve the dynamic range of the detector, is being planned. As the minimal detectability of the element can be calculated without scatter radiation by the noise due to the photon counting statistics in CT (Chasler *et al.*,

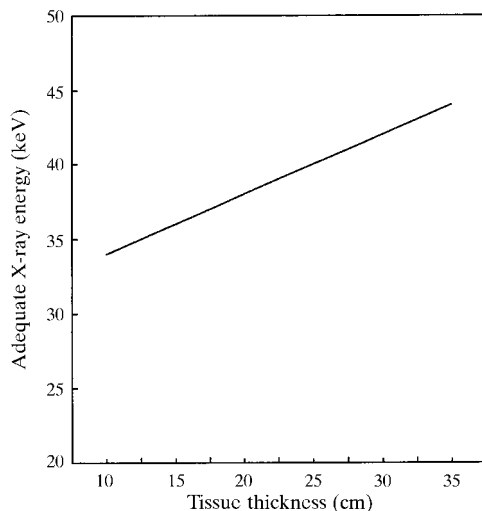


Figure 4

Relationship between adequate X-ray energy and body thickness. At the 20 cm body thickness of human chest, about 37 keV is the most adequate X-ray energy to image the coronary artery. X-ray exposure to the patients would be reduced at this higher X-ray energy than that just above the *K*-edge energy without reducing the image contrast.



Figure 5

High-spatial-resolution CT image of a rat skull. The structures of the nasal cartilage can be observed at 36 μm spatial resolution.

1977), the relationship between the minimal detectability of iodine and photon flux density can be calculated (Fig. 6).

Using a linear-array detector composed of high-purity germanium or CdWO_4 scintillator/diode, Dilmanian *et al.* at Brookhaven National Laboratory constructed a highly sensitive synchrotron radiation CT system to generate a map of the distribution of low- and intermediate-Z elements (*i.e.* P, S, Cl, K, Ca and Fe) for neurological diagnosis (Dilmanian *et al.*, 1991, 1997; Wu *et al.*, 1995).

3.2. Fluorescent X-ray CT

Fluorescent X-ray analysis is commonly used to detect very low concentrations of elements of the order of picograms, but these measurements require thin specimen slices scanned perpendicular to the surface. The first fluorescent tomogram using X-ray tubes demonstrated a 0.5% iodine solution in a volume of $2.5 \times 2.6 \times 2.5$ mm (Cesareo & Mascarenhas, 1989), and micro-tomography with synchrotron radiation showed iron in the head of a bee (Boisseau & Grodzins, 1987). In Japan, fluorescent tomography with synchrotron radiation has been performed since 1993, and can detect about 200 ng of iodine in a 4 mm^3 volume (Takeda, Ito *et al.*, 1994; Takeda, Maeda *et al.*, 1995, 1996; Maeda, *et al.*, 1997).

Since 1995, fluorescent X-ray CT (FXCT) using a parallel collimator is being developed to detect non-radioactive contrast materials (high-Z elements) in living specimens (Takeda, Akiba *et al.*, 1996; Takeda, Yuasa *et al.*, 1997; Yuasa, Akiba, Takeda, Kazama *et al.*, 1997; Akiba *et al.*, 1997). Now, images similar to those obtained by radionuclide examinations have been obtained with single-photon-emission computed tomography (SPECT). The FXCT system consists of an Si(111) double monochromator, an X-ray slit and a collimator for detection, a

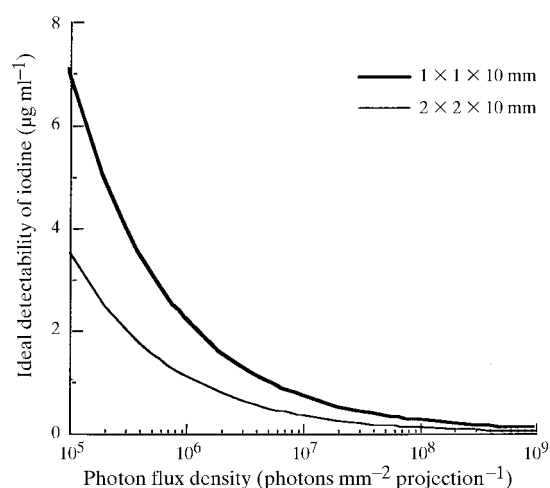


Figure 6

Minimal detectability of iodine corresponding to the photon flux density in front of the detector by synchrotron radiation X-ray CT. Less than $3 \mu\text{g ml}^{-1}$ iodine can be imaged at 1 mm spatial resolution with 10 mm slice thickness, $10^6 \text{ photons mm}^{-2}$ projection $^{-1}$ and 180 projections.

scanning table for the target organ and a highly purified germanium (HPGe) detector for fluorescent X-rays (Fig. 7). The energy of the monochromatic X-ray beam was adjusted to 37.0 keV. The monochromatic X-ray beam was collimated into 1×1 mm (horizontal and vertical, respectively). In the detecting portion, excited fluorescent X-rays were collimated to 1×30 mm with length 100 mm. A five-hole phantom filled with iodine solution (50, 100, 200, $500 \mu\text{g ml}^{-1}$) was imaged. Attenuation correction of the $K\alpha$ line at each projection was performed by transmission CT image data. FXCT images were reconstructed using a filtered-back projection method.

In every 20 s, the spectrum of the HPGe detector showed the $K\alpha$ and $K\beta$ peaks of fluorescent X-rays, Compton scattering and Thomson scattering for an excited iodine content of less than $1 \mu\text{g}$. The five holes filled with iodine solution could be demonstrated clearly (Fig. 8), whereas the transmission CT image could not detect the iodine solution. Observation of the $50 \mu\text{g ml}^{-1}$ iodine solution indicated that the excited iodine content in the measured voxel was about 50 ng ($50 \mu\text{g ml}^{-1} \times 1 \times 10^{-3} \text{ ml}$). The minimal detectable concentration of iodine solution was calculated as 30 ng by the least-squares method. FXCT provided excellent spatial resolution in imaging non-radioactive low-contrast material, comparable with that of SPECT, but correction for X-ray absorption by the object is indispensable to demonstrate the regional distribution of the contrast element quantitatively.

3.3. Scattered X-ray CT

Scattered X-rays in the target materials also convey information about the materials. The scattering consists of coherent (Thomson) and incoherent (Compton) modes. At small angles, coherent scattering X-rays are observed, where the angle corresponds to the specific materials. This phenomena can be applied to biomedical materials (Clark & Van Dyk, 1973), whereas the incoherent scattering component can describe electron density of biomedical objects (Lale, 1959). By these principles, we constructed prototypes of coherent scatter CT (CSCT) and incoherent scatter CT (ISCT) and experiments were carried out at the bending-magnet beamline BLNE-5A at KEK.

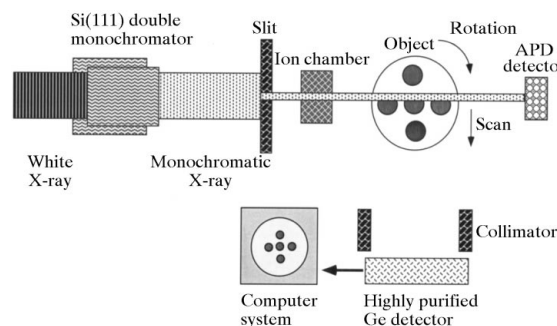


Figure 7

Schematic diagram of fluorescent X-ray CT.

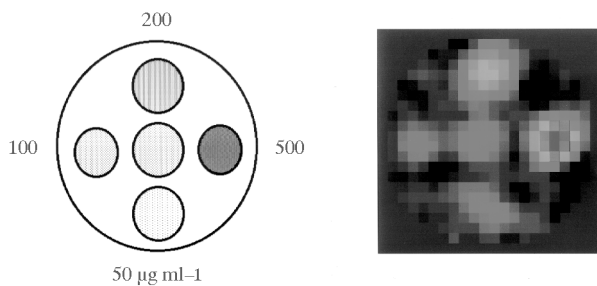


Figure 8

Fluorescent X-ray CT image of phantom. About 50 ng iodine in a volume of 1 mm^3 can be revealed ($50 \mu\text{g ml}^{-1} \times 1 \times 10^{-3} \text{ ml}$).

The preliminary experiment of CSCT with an HPGe detector demonstrated that the subtraction of two images obtained from different scatter angles yielded specific material distribution, and a new system with a scintillator-CCD is under construction for attenuation correction by simultaneously obtained transmission CT (TCT) (Hoshino *et al.*, 1996). On the other hand, the experiment on ISCT succeeded in obtaining a reasonable reconstructed image with the same method as FXCT, after determination of optimal experimental conditions by computer simulation (Yuasa *et al.*, 1996; Yuasa, Akiba, Takeda, Hoshino *et al.*, 1997).

Thus, we are now developing a multi-CT system with CSCT, ISCT, FXCT and TCT to accomplish attenuation correction and complete description of target organs.

3.4. Phase-contrast X-ray CT

The present X-ray images were obtained from the difference in X-ray absorption due to the X-ray linear attenuation coefficient. To improve the image contrast without contrast material, we have been studying phase-contrast imaging using synchrotron X-rays and an interferometer (Momose & Fukuda, 1995; Takeda, Momose *et al.*, 1995). Phase-contrast X-ray CT (Momose, 1995) could clearly demonstrate rabbit cancer (Momose, Takeda & Itai, 1995; Momose *et al.*, 1996) and human breast tumor (Takeda, Momose *et al.*, 1998). Details of phase CT and future development plans are described by Momose *et al.* (1998).

4. Conclusions

Several attempts in Japan to apply synchrotron radiation to biomedical have been briefly introduced. In particular, aortographic CAG and fluorescent X-ray CT are quite important prospective clinical applications. Phase-contrast X-ray CT is an interesting challenge which is expected to improve the precision of the 'X-ray eye'.

We thank M. Akisada MD for his clinical advice, S. Ohtsuka MD, Y. Sugishita MD and S. Tada MD for their

help in clinical applications, K. Umetani PhD, S. Matsushita MD, T. Doi MD and J. Echigo MD for their help in the animal experiments of 2D-CAG, and T. Yuasa PhD, A. Uchida and several postgraduate students for their help in system development. These experiments were performed under the approval of the Photon Factory Program Advisable Committee (proposal Nos. 95G245, 95G289). These researches were partially supported by a Grant-in-Aid for Scientific Research (Nos. 05404037, 08407024, 03670538) and for Developmental Science Research (No. 06507002), from the Ministry of Education, Science, Sports and Culture.

References

- Akiba, M., Takeda, T., Yuasa, T., Uchida, A., Hyodo, K., Akatsuka, T. & Itai, Y. (1997). *Jpn. J. Med. Electron. Biol. Eng.* **35**(4), 303–312. (Abstract in English.)
- Akisada, M., Ando, M., Hyodo, K., Hasegawa, S., Konishi, K., Nishimura, K., Maruhashi, A., Toyofuku, F., Suwa, A. & Kohra, K. (1986). *Nucl. Instrum. Methods*, **A246**, 713–718.
- Boisseau, P. & Grodzins, L. (1987). *Hyperfine Interact.* **33**, 283–292.
- Bonse, U. & Busch, F. (1996). *Prog. Biophys. Mol. Biol.* **65**(1/2), 133–169.
- Cesareo, R. & Mascarenhas, S. (1989). *Nucl. Instrum. Methods*, **A277**, 669–672.
- Chapman, D., Thomlinson, W. C., Gmur, N. F., Dervan, J. P., Stavola, T., Giacomini, J., Gordon, H., Rubenstein, E., Lavender, W., Schulze, C. & Thompson, A. C. (1995). *Rev. Sci. Instrum.* **66**, 1329–1331.
- Chasler, D. A., Riederer, S. J. & Pelc, N. J. (1977). *J. Comput. Assist. Tomogr.* **1**(1), 64–74.
- Clark, R. L. & Van Dyk, G. (1973). *Phys. Med. Biol.* **18**(4), 532–539.
- Dilmanian, F. A., Garrett, R. F., Thomlinson, W. C., Berman, L. E., Chapman, L. D., Hasting, J. B., Luke, P. N., Oversluisen, T., Siddons, D. P., Slatkin, D. N., Stojanoff, V., Thompson, A. C., Volkow, N. D. & Zeman, H. D. (1991). *Nucl. Instrum. Methods*, **B56/57**, 1208–1213.
- Dilmanian, F. A., Wu, X. Y., Parsons, E. C., Ren, B., Kress, J., Button, T. M., Chapman, L. D., Coderre, J. A., Giron, F., Greenberg, D., Krus, D. J., Liang, Z., Marcovici, S., Petersen, M. J., Roque, C. T., Shleifer, M., Slatkin, D. N., Thomlinson, W. C., Yamamoto, K. & Zhong, Z. (1997). *Phys. Med. Biol.* **42**, 371–387.
- Dix, W. R. (1995). *Synchrotron Rad. News*, **8**, 38.
- Dix, W. R., Engelke, K., Graeff, W., Hamm, C., Heuer, J., Kaempf, W., Kupper, W., Lohmann, M., Reime, B. & Reumann, R. (1992). *Nucl. Instrum. Methods*, **A314**, 307–315.
- Fukagawa, H., Noda, C., Suzuki, Y., Hasagawa, S., Ando, M., Hyodo, K., Nishimura, K., Akisada, M., Takenaka, E., Hosaka, R. & Toyohuku, F. (1989). *Rev. Sci. Instrum.* **60**, 2268–2271.
- Grodzins, L. (1983). *Nucl. Instrum. Methods*, **206**, 541–545.
- Hessel, S. J. (1983). *Complications of Angiography and Other Catheter Procedures in Abrams Angiography*, pp. 1041–1056. Boston, MA: Little, Brown & Co.
- Hoshino, A., Takeda, T., Akiba, M., Kazama, M., Watanabe, Y., Yuasa, T., Hyodo, K., Uchida, A., Akatsuka, T. & Itai, Y. (1996). *Proc. 18th Annu. Int. Conf. IEEE Eng. Med. Biol.* CD-ROM #627.
- Hyodo, K., Nishimura, K. & Ando, M. (1991). *Handbook on Synchrotron Radiation*, Vol. 4, edited by S. Ebashi, M. Koch & E. Rubenstein, pp. 55–94. Amsterdam: North Holland.

- Hyodo, K., Shiwaku, H., Yamamoto, S., Kitamura, H. & Ando, M. (1994). *Synchrotron Radiation in the Biosciences*, edited by B. Chance, J. Deisenhofer, S. Ebashi, T. Goodhead, J. R. Helliwell, H. E. Huxley, T. Izuka, J. Kirz, T. Mitsui, E. Rubenstein, N. Sakabe, T. Sasaki, G. Schmahl, H. B. Stuhmann, K. Wuttrich & G. Zaccai, pp. 653–664. Oxford University Press.
- Itai, Y., Takeda, T., Akatsuka, T., Maeda, T., Hyodo, K., Uchida, A., Yuasa, T., Kazama, M., Wu, J. & Ando, M. (1995). *Rev. Sci. Instrum.* **66**(2), 1385–1387.
- Kazama, M., Takeda, T., Akiba, M., Yuasa, T., Hyodo, K., Ando, M., Akatsuka, T. & Itai, Y. (1997). *Med. Imag. Tech.* **15**, 615–624.
- Lale, P. G. (1959). *Phys. Med. Biol.* **4**, 156–167.
- Maeda, T., Takeda, T., Hyodo, K., Akatsuka, T., Yuasa, T., Uchida, A., Hiranaka, Y. & Itai, Y. (1997). *Jpn. J. Med. Electron. Biol. Eng.* **35**(2), 158–166. (Abstract in English.)
- Momose, A. (1995). *Nucl. Instrum. Methods*, **A352**, 622–628.
- Momose, A. & Fukuda, J. (1995). *Med. Phys.* **22**, 375–379.
- Momose, A., Takeda, T. & Itai, Y. (1995). *Rev. Sci. Instrum.* **66**, 1434–1436.
- Momose, A., Takeda, T., Itai, Y. & Hirano, K. (1996). *Nature Med.* **2**, 473–475.
- Momose, A., Takeda, T., Itai, Y., Yoneyama, A. & Hirano, K. (1998). *J. Synchrotron Rad.* **5**, 309–314.
- Mori, H., Hyodo, K., Tobita, K., Chujo, M., Shinozaki, Y., Sugishita, Y. & Ando, M. (1994). *Circulation*, **89**, 863–871.
- Motz, J. W. & Danos, M. (1978). *Med. Phys.* **5**, 8–22.
- Ohtsuka, S., Sugishita, Y., Takeda, T., Itai, Y., Hyodo, K. & Ando, M. (1997). *Jpn. Circ. J.* **61**, 432–440.
- Pepine, C. J., Allen, H. D., Bashore, T. M., Brinker, J. A., Cohn, L. H., Dillon, J. C., Hillis, L. D., Klocke, F. J., Parmley, W. W., Ports, T. A., Rapaport, E., Ross, J. Jr, Rutherford, B. D., Ryan, T. J. & Scanlon, P. J. (1991). *J. Am. Collect. Cardiol.* **18**, 1149–1182.
- Rubenstein, E., Hofstadter, R., Zeman, H. D., Thompson, A. C., Otis, J., Brown, G. S., Giacomini, J. C., Gordon, H. J., Kernoff, R. S., Harrison, D. C. & Thomlinson, W. (1986). *Proc. Natl Acad. Sci. USA*, **83**, 9724–9728.
- Rubenstein, E., Hughes, E. B., Campbell, L. E., Hofstadter, R., Kirk, R. L., Krolicki, T. J., Stone, J. P., Wilson, S., Zeman, H. D., Brody, W. R., Macovski, A. & Thompson, A. C. (1981). *SPIE*, **314**, 42–48.
- Takeda, T., Akatsuka, T., Hyodo, K., Hiranaka, Y., Zeniya, T., Yuasa, T., Sato, M., Wu, J., Ishikawa, N. & Itai, Y. (1992). *Med. Imag. Tech.* **10**, 299–300.
- Takeda, T., Akiba, M., Yuasa, T., Akatsuka, T., Kazama, M., Hoshino, Y., Hyodo, K., Dilmanian, F. A., Akatsuka, T. & Itai, Y. (1996). *SPIE*, **2708**, 685–695.
- Takeda, T., Akisada, M., Nakajima, T., Umetani, K., Ueda, K. & Yamaguchi, C. (1990). *J. Cardiovasc. Technol.* **9**, 203–211.
- Takeda, T., Itai, Y., Hayashi, K., Nagata, Y., Yamaji, H. & Hyodo, K. (1994). *J. Comput. Assist. Tomogr.* **18**, 98–101.
- Takeda, T., Itai, Y., Wu, J., Ohtsuka, S., Hyodo, K., Ando, M., Nishimura, K., Hasegawa, S., Akatsuka, T. & Akisada, M. (1995). *Acad. Radiol.* **2**, 602–608.
- Takeda, T., Itai, Y., Yoshioka, H., Umetani, K., Ueda, K. & Akisada, M. (1994). *Med. Biol. Eng. Comput.* **32**, 462–468.
- Takeda, T., Ito, K., Kishi, K., Maeda, T., Yuasa, T., Wu, J., Kazama, M., Hyodo, K., Akatsuka, T. & Itai, Y. (1994). *Med. Imag. Tech.* **12**, 537–538.
- Takeda, T., Kazama, M., Zeniya, T., Yuasa, T., Akiba, M., Uchida, A., Hyodo, K., Akatsuka, T., Ando, M. & Itai, Y. (1998). *Medical Application with Synchrotron Radiation*, edited by M. Ando & C. Uyama. Berlin: Springer Verlag. In the press.
- Takeda, T., Maeda, T., Yuasa, T., Akatsuka, T., Ito, K., Kishi, K., Wu, J., Kazama, M., Hyodo, K. & Itai, Y. (1995). *Rev. Sci. Instrum.* **66**(2), 1471–1473.
- Takeda, T., Maeda, T., Yuasa, T., Akatsuka, T., Ito, K., Kishi, K., Wu, J., Kazama, M., Hyodo, K. & Itai, Y. (1996). *Med. Imag. Tech.* **14**, 183–194.
- Takeda, T., Momose, A., Itai, Y., Wu, J. & Hirano, K. (1995). *Acad. Radiol.* **2**, 799–803.
- Takeda, T., Momose, A., Ueno, E. & Itai, Y. (1998). *J. Synchrotron Rad.* **5**, 1133–1135.
- Takeda, T., Umetani, K., Doi, T., Echigo, J. & Itai, Y. (1998). *Medical Application with Synchrotron Radiation*, edited by M. Ando & C. Uyama. Berlin: Springer Verlag. In the press.
- Takeda, T., Umetani, K., Doi, T., Echigo, J., Ueki, H., Ueda, K. & Itai, Y. (1997). *Acad. Radiol.* **4**, 438–445.
- Takeda, T., Yuasa, T., Hoshino, A., Akiba, M., Uchida, A., Kazama, M., Hyodo, K., Dilmanian, F. A., Akatsuka, T. & Itai, Y. (1997). *SPIE*, **3149**, 160–172.
- Umetani, K., Ueda, K., Takeda, T., Itai, Y., Akisada, M. & Nakajima, T. (1993). *Nucl. Instrum. Methods*, **A335**, 569–579.
- Umetani, K., Ueki, H., Ueda, K., Hirai, T., Takeda, T., Doi, T., Wu, J., Itai, Y. & Akisada, M. (1996). *J. Synchrotron Rad.* **3**, 136–144.
- Wu, X. Y., Dilmanian, F. A., Chen, Z., Ren, B., Slatkin, D. N., Chapman, D., Shleifer, M., Staicu, F. A. & Thomlinson, W. (1995). *Rev. Sci. Instrum.* **66**, 1346–1347.
- Yuasa, T., Akiba, M., Takeda, T., Hoshino, Y., Watanabe, Y., Hyodo, K., Dilmanian, F. A., Akatsuka, T. & Itai, Y. (1997). *IEEE Trans. Nucl. Sci.* **44**, 1760–1769.
- Yuasa, T., Akiba, M., Takeda, T., Kazama, M., Hoshino, Y., Watanabe, Y., Hyodo, K., Dilmanian, F. A., Akatsuka, T. & Itai, Y. (1997). *IEEE Trans. Nucl. Sci.* **44**, 54–62.
- Yuasa, T., Takeda, T., Akiba, M., Hoshino, A., Watanabe, Y., Hyodo, K., Dilmanian, F. A., Akatsuka, T. & Itai, Y. (1996). *Proc. 18th Annu. Int. Conf. IEEE Eng. Med. Biol.* CD-ROM #181.
- Zeniya, T., Takeda, T., Hyodo, K., Yuasa, T., Uchida, A., Maeda, T., Wu, J., Hiranaka, Y., Akatsuka, T. & Itai, Y. (1997). *Med. Imag. Tech.* **15**, 121–137.